
Mamba in Speech: Towards an Alternative to Self-Attention

Xiangyu Zhang^{1*}, Qiquan Zhang^{1*}, Hexin Liu^{2*}, Tianyi Xiao³,
Xinyuan Qian⁴, Beena Ahmed¹, Eliathamby Ambikairajah¹, Haizhou Li^{5,6}, Julien Epps¹

¹The University of New South Wales, ²Nanyang Technological University,

³Beijing Institute of Technology ⁴University of Science and Technology Beijing

⁵National University of Singapore, ⁶The Chinese University of Hong Kong, Shenzhen

Abstract

Transformer and its derivatives have achieved success in diverse tasks across computer vision, natural language processing, and speech processing. To reduce the complexity of computations within the multi-head self-attention mechanism in Transformer, Selective State Space Models (i.e., Mamba) were proposed as an alternative. Mamba exhibited its effectiveness in natural language processing and computer vision tasks, but its superiority has rarely been investigated in speech signal processing. This paper explores solutions for applying Mamba to speech processing using two typical speech processing tasks: speech recognition, which requires semantic and sequential information, and speech enhancement, which focuses primarily on sequential patterns. The results exhibit the superiority of bidirectional Mamba (BiMamba) for speech processing to vanilla Mamba. Moreover, experiments demonstrate the effectiveness of BiMamba as an alternative to the self-attention module in Transformer and its derivatives, particularly for the semantic-aware task. The crucial technologies for transferring Mamba to speech are then summarized in ablation studies and the discussion section to offer insights for future research.¹

1 Introduction

Transformer-based models [1] have shone brightly across various domains in machine learning, including computer vision (CV) [2–4], natural language processing (NLP) [5–7], and speech processing [8, 9]. This success is linked to the multi-head self-attention (MHSA) module, which facilitates the representation of intricate data structures within a specific context window. However, the self-attention mechanism encounters a challenge with computational complexity, which grows quadratically as the size of the context window increases. In speech tasks, the window typically encompasses an entire speech sample. This particularly yields an extensive context especially for frame-level acoustic feature sequences, leading to a considerable increase in computational complexity. Numerous efforts have been made to address this challenge, with one notable approach being the utilization of a state space model (SSM). SSM-based approaches [10–13] have been developed to handle sequential data across diverse tasks and modalities. By integrating a time-varying mechanism into SSMs, a new model named Mamba [14] has been proposed and shown outstanding performance in CV [15, 16] and NLP [17].

However, in the field of speech processing, despite some attempts to replace transformers with Mamba [18–20], the results have not been as satisfactory as expected. In [18], each Mamba is directly employed as a substitute for a Transformer within a dual-path framework for speech separation. [19] proposed SPMamba for speech separation, where Mamba is used in conjunction with MHSA.

¹Code will be public once accepted

Although these approaches achieve high performance by employing a dual-path strategy or combining Mamba with attention to form a new module, these methods negate the low time complexity of Mamba. In the domain of multi-channel speech enhancement, Mamba was implemented to enhance a SpatialNet from offline to online [20] yet underperformed the vanilla version. Since different speech tasks focus on various characteristics of a speech signal (e.g., speaker, language, emotion), they generally require different levels of information. However, existing approaches have mostly investigated speech enhancement and separation tasks, which focus primarily on the low-level information within a speech signal. Therefore, it is still unclear how to efficiently employ Mamba for other speech tasks, such as speech recognition and spoken language understanding, which require high-level semantic information within the speech signal.

In this paper, we provide solutions for applying Mamba to different speech tasks based on their varying information requirements (in different abstraction levels [21]) using speech recognition and speech enhancement as examples. Our research first proposes and compares two bidirectional Mamba (BiMamba) structures, being external BiMamba (ExtBiMamba) and inner BiMamba (InnBiMamba). Experiments suggest that a bidirectional design can enhance the capability of Mamba to model global dependencies within the features of a speech signal. Mamba and BiMamba models are then evaluated independently or as replacements for MHSA in Transformer and Conformer models across multiple datasets. We demonstrate that the proposed BiMamba modules require additional nonlinearity to learn high-level semantic information in speech tasks, serving as an alternative to MHSA is thus an optimal approach to apply Mamba in this scenario.

2 Preliminary

The State Space Model (SSM) based approaches, including the Structured State Space Sequence Model (S4) [11] and Mamba [14], are derived from continuous systems. S4 facilitates the transformation of a one-dimensional function or sequence, $x(t) \in \mathbb{R}$ to $y(t) \in \mathbb{R}$, through an intermediate state $h(t)$ in \mathbb{R}^n . The process leverages A from $\mathbb{R}^{n \times n}$ as the evolution matrix and B from $\mathbb{R}^{D \times N}$, C from $\mathbb{R}^{D \times N}$ as the input and output mapping matrices, respectively.

The fundamental equations are represented as:

$$h'(t) = Ah(t) + Bx(t), \quad y(t) = Ch(t) + Dx(t). \quad (1)$$

In their discrete forms, parameter D can be represented as the residual connection in Neural Network, S4 and Mamba introduce a scaling parameter Δ , transforming the continuous matrices A, B into the discrete matrices \tilde{A}, \tilde{B} respectively. This transformation commonly utilizes the Zero-Order Hold (ZOH) method, defined by:

$$\tilde{A} = \exp \Delta A, \quad \tilde{B} = (\Delta A)^{-1}(\exp \Delta A - I)\Delta B. \quad (2)$$

Consequently, with the discretization into \tilde{A}, \tilde{B} , the equation (1) is adjusted for a discrete timestep Δ , given as:

$$h_t = \tilde{A}h_{t-1} + \tilde{B}x_t, \quad y_t = Ch_t. \quad (3)$$

The model then computes the final output from convolution via

$$y = x * \bar{K}, \quad \bar{K} = (C\tilde{B}, C\tilde{A}\tilde{B}, \dots, C\tilde{A}^{L-1}\tilde{B}) \quad (4)$$

The A matrix, as described above, is commonly initialized with a HiPPO matrix [22] or a Diagonal matrix [12] to adeptly capture long-range dependencies. Mamba enhances S4 by integrating a time-varying mechanism, which enlarges the dimensions of matrices B and C to $\mathbb{R}^{B \times L \times N}$, and modifies \tilde{A} and \tilde{B} to $\mathbb{R}^{B \times L \times D \times N}$.

Although these modifications have enhanced model performance, granting it "selective" capabilities, they do not alter the inherent nature of SSMs, which operate in a unidirectional manner such as RNNs [23, 24]. This is not an issue in training large language models, as many of these models are trained in an autoregressive manner [25, 26]. However, for non-autoregressive speech models, we require a module with causal capabilities similar to attention. Thus, finding a suitable method to address this issue is essential. Moreover, the observation that Mamba's A matrix randomization and real-valued diagonal initialization perform equivalently suggests that Mamba's ability to delineate dependencies between inputs, compared to S4, needs further enhancement.

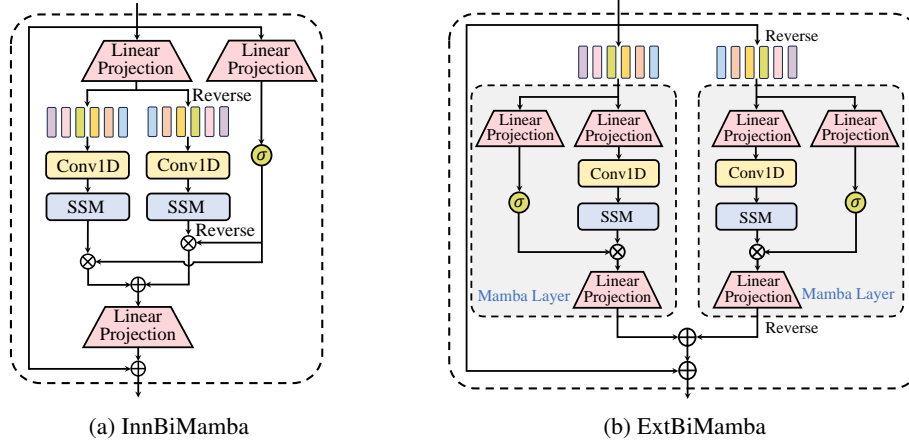


Figure 1: The illustrations of (a) inner bidirectional Mamba (InnBiMamba) [15], and (b) the external bidirectional Mamba (ExtBiMamba). σ denotes the SiLU activation.

3 Investigating Mamba in Speech Processing

3.1 Bidirectional processing

The original Mamba performs causal computations in a unidirectional manner, using only historical information. However, in speech tasks, the model is provided with the complete speech signal. Therefore, Mamba requires bidirectional computations, as employed in the MHSA module, to capture global dependencies within the features of the input signal. In this paper, we explored two bidirectional strategies for Mamba in speech tasks, i.e., inner bidirectional Mamba (InnBiMamba) [15] and external bidirectional Mamba (ExtBiMamba) as shown in Figure 2.

Inner Bidirectional Layer (InnBiMamba). We first explore the inner bidirectional Mamba (InnBiMamba) [15] for speech tasks as detailed in Figure 1a. Here, two SSM modules share the same input and output projection layers. The process feeds the input forward into one SSM module, while reversing the input along the time dimension before feeding it into the other SSM module. The output of the backward SSM module is reversed back before being combined with the output of the forward SSM module. The combined output then passes through the output projection layer.

External Bidirectional Layer (ExtBiMamba). In addition, we also propose a simpler and more straight bidirectional modeling strategy, i.e., external bidirectional Mamba (ExtBiMamba). Unlike the InnBiMamba layer, the ExtBiMamba layer involves different input and output projection layers in forward and backward Mamba layers, respectively, as illustrated in Figure 1b. The input is fed into the forward Mamba layer and the backward Mamba layer processes the reversed input. The outputs of two Mamba layers are fused with addition operation and a residual connection is applied around the ExtBiMamba layer. Please refer to Appendix A for detailed descriptions of two algorithms.

3.2 Task-aware model designs

Recent works have investigated Mamba in speech separation and speech enhancement. These tasks primarily focus on low-level spectral information of a speech signal [27]. In contrast, other speech tasks like speech recognition and spoken language understanding require capturing high-level semantic information. With reference to equation 3, SSM comprises mostly linear computations. This implies that it has limited capability to capture high-level information such as semantics and emotions. Although SiLU is used within residual structures in practical implementations, this is primarily to represent the parameter D in equation 1 for the state space model [14]. Therefore, adding more nonlinearity ability is crucial for Mamba to capture high-level information.

To capture information of various abstraction levels, we progressively explored three structures for increasing nonlinearity capability. As depicted in Figure 2a, the first strategy uses the Mamba/BiMamba layers independently (i.e., as a direct replacement for the transformer layer) to construct the Mamba/BiMamba model. The second approach employs the Mamba/BiMamba layer to replace the

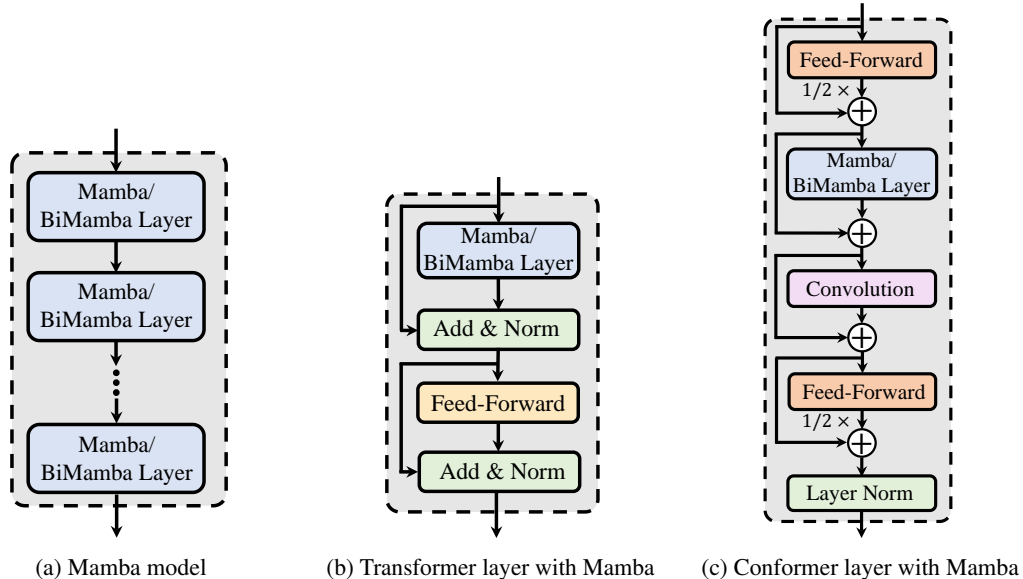


Figure 2: Three applications of the Mamba layer in speech processing include: (a) using stacked unidirectional/bidirectional Mamba layers as an alternative to Transformer layers; (b) replacing causal and non-causal MHSA in Transformer layers with unidirectional/bidirectional Mamba; and (c) integrating the Mamba layer into the Conformer layer, as shown in Fig. 2b.

MHSA modules within the Transformer, where the feed-forward net (FFN) and layernorm modules are used to provide nonlinearity. The third replaces the MHSA modules with Mamba/BiMamba layers in the Conformer, which is a variant of the Transformer employing a convolutional layer after each MHSA designed to additionally capture local information.

4 Experimental Setup

4.1 Speech Enhancement

Datasets. We follow the studies [28, 29] and employ the clean speech clips from LibriSpeech *train-clean-100* corpus [30] for training, comprising 28 539 clips spoken by 251 speakers. The noise recordings are collected from the following datasets [31], i.e., the noise data of the MUSAN datasets [32], the RSG-10 dataset [33] (*voice babble*, *F16*, and *factory welding* are excluded for testing), the Environmental Noise dataset [34, 35], the colored noise set (with an α value ranging from -2 to 2 in increments of 0.25) [36], the UrbanSound dataset [37] (*street music* recording no 26 270 is excluded for testing), the QUT-NOISE dataset [38], and the Nonspeech dataset [39]. Please refer to Appendix C.1 for the detailed experiment setup.

Model Configurations. In our experiments, we employ the same backbone network architecture (a typical neural solution to speech enhancement) [31, 29, 40, 41], which comprises an input embedding layer, stacked feature transformation layers (such as Mamba, Transformer, and Conformer layers), and an output layer. To systematically study the Mamba networks, we use the standard Transformer [31, 29] and Conformer [8] models as the baseline backbone networks, across causal and non-causal configurations. Please refer to the Appendix C.1 for detailed model configurations.

We evaluated enhanced speech with five commonly used assessment metrics, i.e, perceptual evaluation of speech quality (PESQ) [42], extended short-time objective intelligibility (ESTOI), and three composite metrics. For PESQ, both wide- and narrow-band PSEQ were used to evaluate the speech quality, with the score range of $[-0.5, 4.5]$. The ESTOI [43] score is typically between 0 and 1. The three composite metrics [44] are used to predict the mean opinion scores of the intrusiveness of background noise (CBAK), the signal distortion (CSIG), and the overall signal quality (COVL), respectively, with the score range of $[0, 5]$. For all these five metrics, a higher score means better performance.

4.2 Speech Recognition

Datasets. We evaluate our models on ASR with four datasets, i.e., LibriSpeech [30], AN4 [45], SEAME [46], and ASRU [47], in which all speech signals are sampled at 16 kHz. LibriSpeech (LibriSpeech960) containing approximately 1000 hours of audio recordings and their paired texts, in which a subset LibriSpeech100 is used for ablation studies due to its higher recording quality. The AN4 dataset contains approximately one hour of audio recordings of primarily spoken alphanumeric strings, such as postal codes and telephone numbers. It is employed to assess the model’s ability to perform with a small dataset. Two English-Mandarin code-switching datasets SEAME and ASRU-CS-2019 (denoted as ASRU) are then used for a more challenging scenario compared to monolingual. The SEAME dataset contains 200-hour spontaneous South-east Asian-accented speech with intra- and inter-sentential code-switches, divided as introduced in [48]. The ASRU dataset contains a 500-hour Mandarin and a 200-hour code-switching training sets recorded in mainland China, where only the code-switching set is used for training, following [46, 47, 49].

Model Configurations. We employed the best-performing Conformer/Transformer model configurations provided by official recipes in ESPnet or existing works. We maintained the experimental setups of models related to Mamba the same as Conformer/Transformer. The substitution of MHSA modules with Mamba/BiMamba is merely implemented within the encoder layers of a joint CTC-Attention model [50], where Transformer decoder layers serve as the ASR decoder. Detailed model configurations are in Appendix B.

We employ word error rate (WER) and mixed word error rate (MER) to measure the ASR performance for monolingual and code-switching ASR tasks, respectively, where the MER considers the word error rate for English and the character error rate for Mandarin. All experiments are performed using the ESPnet toolkit [51].

5 Experimental Results and Analysis

5.1 Speech Enhancement (Also c.f. Appendix C.2)

InnBiMamba vs. ExtBiMamba. In Table 1, we illustrate the comparison results of InnBiMamba and ExtBiMamba across different model sizes, in terms of six metrics, i.e., NB-PESQ, WB-PESQ, ESTOI, CSIG, CBAK, and COVL. Overall, ExtBiMamba consistently performs slightly better than InnBiMamba across the model sizes. In addition, Table 2 compares the training speed (training time per step) and inference speed (real-time factor [52]) of InnBiMamba and ExtBiMamba, confirming the superiority of ExtBiMamba over InnBiMamba. Real-time factor (RTF) is measured by dividing the time taken to process a speech utterance by the duration of the speech. The RTFs were measured on an NVIDIA Tesla V100 GPU and averaged over 20 executions. We used a batch size of 4 noisy mixtures, each with a duration of 10 seconds [52].

Table 1: Comparison results of InnBiMamba and ExtBiMamba architectures in NB-PESQ, WB-PESQ, ESTOI (%), CSIG, CBAK, and COVL. The BiMamba models are denoted as “Inn/ExtBiMamba-the number of BiMamba layers”.

Method	#Params	Causality	Metrics					
			NB-PESQ	WB-PESQ	ESTOI	CSIG	CBAK	COVL
Noisy	–	–	1.88	1.24	56.12	2.26	1.80	1.67
InnBiMamba-9	4.48 M	✗	2.84	2.14	75.74	3.39	2.59	2.74
ExtBiMamba-5	4.51 M	✗	2.86	2.15	76.12	3.46	2.60	2.78
InnBiMamba-13	6.41 M	✗	2.90	2.19	76.89	3.50	2.63	2.82
ExtBiMamba-7	6.26 M	✗	2.90	2.20	77.04	3.54	2.64	2.84

Table 2: Evaluation results of InnBiMamba and ExtBiMamba in training speed (training time per step) and inference speed (RTF).

	InnBiMamba-9	ExtBiMamba-5	InnBiMamba-13	ExtBiMamba-7
sec/step	0.159	0.122	0.212	0.159
RTF	1.88×10^{-4}	1.69×10^{-4}	2.76×10^{-4}	2.34×10^{-4}

Table 3: Performance comparisons of Transformer and Mamba network architectures in NB-PESQ, WB-PESQ, ESTOI (%), CSIG, CBAK, and COVL, across causal and non-causal configurations. The Transformers with 4 and 6 stacked Transformer layers are denoted as Transformer-4 and Transformer-6, respectively.

Method	#Params	Causality	Metrics					
			NB-PESQ	WB-PESQ	ESTOI	CSIG	CBAK	COVL
Noisy	–	–	1.88	1.24	56.12	2.26	1.80	1.67
Transformer-4	3.29 M	✓	2.56	1.84	70.32	3.17	2.39	2.47
Mamba-4	1.88 M	✓	2.60	1.87	70.99	3.17	2.41	2.48
Mamba-7	3.20 M	✓	2.64	1.91	72.46	3.26	2.45	2.56
Transformer-4	3.29 M	✗	2.74	2.01	73.44	3.31	2.50	2.63
ExtBiMamba-3	2.76 M	✗	2.76	2.05	73.93	3.36	2.53	2.67
ExtBiMamba-4	3.64 M	✗	2.83	2.11	75.43	3.46	2.57	2.75
Transformer-6	4.86 M	✓	2.60	1.87	71.37	3.20	2.41	2.50
Mamba-6	2.76 M	✓	2.63	1.91	71.94	3.23	2.44	2.54
Mamba-10	4.51 M	✓	2.68	1.94	73.20	3.30	2.47	2.59
Transformer-6	4.86 M	✗	2.78	2.05	74.56	3.38	2.52	2.69
ExtBiMamba-5	4.51 M	✗	2.86	2.15	76.12	3.46	2.60	2.78
ExtBiMamba-6	5.39 M	✗	2.88	2.17	76.69	3.50	2.62	2.82

Table 4: Training speed and inference speed of ExtBiMamba and non-causal Transformers.

	Transformer-4	ExtBiMamba-3	ExtBiMamba-4	Transformer-6	ExtBiMamba-5	ExtBiMamba-6
sec/step	0.099	0.089	0.102	0.125	0.122	0.141
RTF	1.48×10^{-4}	1.08×10^{-4}	1.38×10^{-4}	2.12×10^{-4}	1.71×10^{-4}	2.04×10^{-4}

Mamba vs. Transformer. Table 3 compares Transformer and Mamba network architectures. For Mamba models, we report the results of Mamba models with the same number of layers and a similar model size to the Transformer. It can be observed that the Mamba models consistently demonstrate obvious performance superiority over the Transformer models with lower parameter overheads, across causal and noncausal configurations. For instance, the Mamba-7 (3.20 M) and ExtBiMamba-5 (4.51 M) improve on the causal Transformer-4 (3.29 M) and the noncausal Transformer-6 (4.81 M) by 0.08 and 0.08, 0.07 and 0.1, 2.14% and 1.56%, 0.09 and 0.08, 0.06 and 0.08, and 0.09 and 0.09 in terms of NB-PESQ, WB-PESQ, ESTOI, CSIG, CBAK, and COVL, respectively. In addition, ExtBiMamba models provide substantial performance improvements over original (unidirectional) Mamba models across all the metrics, which confirms the effectiveness of the bidirectional modeling. ExtBiMamba-5 (4.51 M) provided gains of 0.18 in NB-PESQ, 0.21 in WB-PESQ, 2.92% in ESTOI, 0.16 in CSIG, 0.13 in CBAK, and 0.19 in COVL over Mamba-10 (4.51 M), respectively.

Mamba vs. Conformer. Table 5 reports the comparative results of Conformer and Mamba. We can see that original Mamba (causal) models outperform causal Conformer models across all metrics while involving fewer parameters. For instance, compared to causal Conformer-6 (9.26 M), Mamba-20 (8.89 M) improves NB-PESQ by 0.04, WB-PESQ by 0.06, ESTOI by 0.68%, CSIG by 0.05, CBAK by 0.05, and COVL by 0.06. It can also be seen that overall, ExtBiMamba models exhibit slightly better or comparable performance to noncausal Conformer models. Similarly, the substantial performance superiority of the bidirectional modeling is observed from evaluation results of ExtBiMamba-6 (5.39) vs. Mamba-13 (5.83M) and ExtBiMamba-10 (8.89 M) vs. Mamba-20 (8.89 M).

Mamba vs. MHSA. We also explore replacing the MHSA with the Mamba layer in Transformer and Conformer. Tables 12-13 present the evaluation results of replacing the MHSA module in Transformer and Conformer with the Mamba layer. Due to space constraints, Tables 12-13 are placed in Appendix C. It can be observed that Transformers substantially benefit from using the Mamba and BiMamba layers. TransMamba-4 and TransExtBiMamba-6 improve over causal Transformer-4 and non-causal Transformer-6 by 0.09 and 0.13 in NB-PESQ, 0.09 and 0.16 in WB-PESQ, 1.96% and 4.04% in ESTOI, 0.07 and 0.22 in CSIG, 0.06 and 0.13 in CBAK, and 0.08 and 0.19 in COVL, respectively. In addition, TransMamba-4 (3.99 M) and TransInnBiMamba-4 (4.17 M) outperform causal Transformer-6 (4.86 M) and non-causal Transformer (4.86 M), respectively, which further confirms the superiority of Mamba layer over MHSA. Among InnBiMamba and ExtBiMamba,

Table 5: Speech enhancement performance comparisons of Conformer and Mamba network architectures in NB-PESQ, WB-PESQ, ESTOI (%), CSIG, CBAK, and COVL, across causal and noncausal configurations. The Conformer models with 4 and 6 Conformer layers are denoted as Conformer-4 and Conformer-6, respectively.

Method	#Params	Causality	Metrics					
			NB-PESQ	WB-PESQ	ESTOI	CSIG	CBAK	COVL
Noisy	–	–	1.88	1.24	56.12	2.26	1.80	1.67
Conformer-4	6.22 M	✓	2.67	1.94	72.78	3.30	2.46	2.59
Mamba-13	5.83 M	✓	2.70	1.97	73.53	3.32	2.50	2.62
Conformer-4	6.22 M	✗	2.88	2.17	76.68	3.51	2.61	2.82
ExtBiMamba-6	5.39 M	✗	2.88	2.18	76.73	3.50	2.62	2.82
ExtBiMamba-7	6.26 M	✗	2.90	2.20	77.04	3.54	2.64	2.84
Conformer-6	9.26 M	✓	2.68	1.94	73.41	3.30	2.46	2.59
Mamba-20	8.89 M	✓	2.72	2.00	74.09	3.35	2.51	2.65
Conformer-6	9.26 M	✗	2.91	2.20	77.56	3.54	2.62	2.84
ExtBiMamba-10	8.89 M	✗	2.91	2.20	77.64	3.59	2.65	2.87

Table 6: Training speed and inference speed of ExtBiMamba and non-causal Conformers.

	Conformer-4	ExtBiMamba-6	ExtBiMamba-7	Conformer-6	ExtBiMamba-10
sec/step	0.160	0.142	0.156	0.215	0.206
RTF	2.27×10^{-4}	2.07×10^{-4}	2.37×10^{-4}	3.27×10^{-4}	3.32×10^{-4}

we observe that TransExtBiMamba performs slightly better than TransInnBiMamba. With fewer parameters, TransExtBiMamba-4 (5.74 M) achieves slightly higher scores in WB-PESQ, CSIG, CBAK, and COVL, but slightly lower scores in NB-PESQ and ESTOI than TransInnBiMamba-6 (6.19 M).

As shown in Table 13, we observe that the Conformer architecture can benefit from the use of Mamba and ExtBiMamba. The ConExtBiMamba-4 and ConExtBiMamba-6 outperform non-causal Conformer-4 and Conformer-6 by 0.04 and 0.02 in NB-PESQ, 0.03 and 0.03 in WB-PESQ, 1.06% and 0.65% in ESTOI, 0.06 and 0.06 in CSIG, 0.03 and 0.03 in CBAK, and 0.06 and 0.05 in COVL, respectively. In addition, ConExtBiMamba-4 (8.67 M) also exhibits a slightly better performance than non-causal Conformer-6 (9.26 M). Among InnBiMamba and ExtBiMamba, similarly, ConExtBiMamba performs better than ConvInnBiMamba.

5.2 Speech Recognition

Independent vs. Substitute for MHSA. Table 7 reports the performance of Mamba when used independently and as a replacement for MHSA across various datasets. We can observe that independent Mamba and BiMamba models exhibit significantly lower performance compared to the Transformer and Conformer models (with the same number of layers). Since the Mamba has fewer parameters when configured with the same number of layers as the Transformer and Conformer, we increased its number of layers (shown in Appendix D.1) to match the number of parameters with the Conformer to further evaluate Mamba for ASR. The performance of Mamba, however, remained undesirable.

In contrast to the independent Mamba/BiMamba, we observe a significant improvement in the ASR task when Mamba/BiMamba is used as a replacement for MHSA. Specifically, replacing MHSA with ExtBiMamba in the Conformer (named ConExtBiMamba) exhibits higher performance than the SOTA performance achieved by Conformer and Branchformer across multiple datasets with the same training setups. Additionally, ConExtBiMamba provides faster training and inference speeds compared to the Conformer model as detailed in Appendix D.3 Table 18. When we replaced MHSA with ExtBiMamba, the number of parameters exceeded that of the original Conformer. To eliminate the possibility that the performance improvement results from the higher number of parameters, we increase the size of Conformer to a similar number of parameters as ConExtBiMamba, and present the results in Table 8. We found that although the Conformer’s performance improves, it still underperforms ConExtBiMamba and ConInnBiMamba, supporting the effectiveness of our approach.

Unidirectional vs. Bidirectional. Tables 7-8 present the evaluation results of unidirectional Mamba and two bidirectional Mamba modules (i.e., InnBiMamba, and ExtBiMamba) with their corresponding

Table 7: ASR results for the different datasets without language model in WER/MER (%). ‘‘ESPnet’’ means the best result reported by ESPnet official or other paper experimented with ESPnet, where the SEAME and ASRU results come from [53, 54, 49].

Method	LibriSpeech-100		LibriSpeech-960		SEAME		ASRU	
	dev	test	dev	test	man	sgc	dev	test
<i>ESPnet</i>								
Conformer	6.3	6.5	2.1	2.4	16.6	23.3	-	12.2
Branchformer	6.1	6.3	2.2	2.4	-	-	-	-
<i>Reproduced Results</i>								
Branchformer	6.3	6.4	2.2	2.4	16.3	23.2	12.5	11.8
Mamba	40.8	40	21.8	22.3	44.5	55.3	38.0	36.3
InnBiMamba	39.6	38.2	21.8	22.5	44.3	55.4	38.4	37.9
ExtBiMamba	38.5	37.7	21.6	22.1	44.4	55.2	38.2	36.8
Transformer	8.0	8.4	2.8	3.2	17.7	24.5	13.7	13.1
- MHSA + Mamba	10.9	11.2	3.2	3.5	20.7	29.5	24.2	23.1
- MHSA + InnBiMamba	8.8	9.4	2.5	3.0	18.4	26.0	20.2	19.5
- MHSA + ExtBiMamba	8.4	8.7	2.5	2.8	17.2	24.3	18.7	18.0
Conformer	6.3	6.5	2.3	2.6	16.9	23.6	12.8	12.2
- MHSA + Mamba	6.6	6.9	2.6	2.9	17.7	24.9	13.5	12.9
- MHSA + InnBiMamba	6.0	6.4	2.1	2.3	17.1	23.8	12.7	12.2
- MHSA + ExtBiMamba	5.9	6.0	2.0	2.3	16.6	23.4	12.3	11.5

Table 8: WER results on LibriSpeech (without external language model) across various parameter counts and frameworks.

Method	Params (M)	dev	dev other	test	test other
<i>LibriSpeech100</i>					
Transformer	29.38	8.0	20.0	8.4	20.2
- MHSA + InnBiMamba	33.32	8.8	23.3	9.4	23.6
- MHSA + ExtBiMamba	40.42	8.4	22.4	8.7	23.1
Conformer Large	42.17	6.2	17.4	6.4	17.3
Conformer	34.23	6.3	17.4	6.5	17.3
- MHSA + InnBiMamba	36.89	6.0	17.4	6.4	17.6
- MHSA + InnBiMamba Large	49.90	6.1	17.3	6.3	17.3
- MHSA + ExtBiMamba	41.59	5.9	17.1	6.0	17.2
<i>LibriSpeech960</i>					
Transformer	99.36	2.8	7.6	3.2	7.5
- MHSA + InnBiMamba	103.35	2.5	7.4	3.0	7.3
- MHSA + ExtBiMamba	110.04	2.5	6.9	2.8	6.9
Conformer	116.15	2.3	5.5	2.6	5.6
- MHSA + InnBiMamba	118.81	2.1	5.6	2.4	5.5
- MHSA + ExtBiMamba	123.51	2.0	5.4	2.3	5.4

model sizes. InnBiMamba and ExtBiMamba provide substantial improvements over Mamba when used as a replacement for the MHSA module within the Transformer and Conformer. This confirms the effectiveness of the bidirectional modeling.

In addition, ExtBiMamba consistently outperforms InnBiMamba across various frameworks and datasets. We next compare ExtBiMamba with Conformer-Large and ConInnBiMamba-Large as shown in Table 8. The results demonstrate that the performance improvement for ASR stems from factors beyond merely an increased number of model parameters.

Ablation Study on ConExtBiMamba. We employ the ConExtBiMamba model, which improves the SOTA result achieved by Branchformer in the ASR task, for ablation studies. Firstly, we found that within the ConExtBiMamba framework, variations in BiMamba’s hyperparameters had little impact on the performance of the model. Secondly, introducing Gaussian Noise to the A matrix within Mamba in ConBiMamba enhances the model’s effectiveness (for a detailed discussion, see Appendix E.1).

We further discovered that within the Conformer structure, the Swish activation and Macaron-style feed-forward layers enhance the performance of ConExtBiMamba. However, positional encoding and dropout had little effect on the model (for a detailed discussion, see Appendix E.2).

We also found that the robustness of the ConExtBiMamba model was much stronger than that of the Conformer, particularly on very small datasets where its performance was more stable. In tests conducted on the AN4 dataset using five random seeds, ConExtBiMamba outperformed the Conformer in every trial. The mean WER for the Conformer was 10.2, while for ConExtBiMamba it was just 4.54, with a WER variance of only 1.1104 compared with the Conformer’s significantly higher variance of 77.71 (for a detailed discussion, see Appendix E.3).

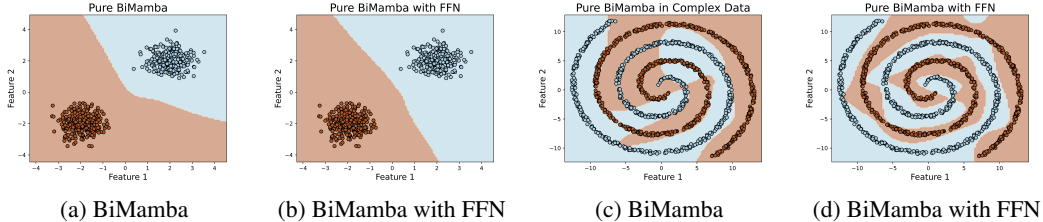


Figure 3: Decision Boundaries for BiMamba and BiMamba with Feed-forward layer(FFN)

6 Discussion

As demonstrated in Section 5.2, independent Mamba or BiMamba models exhibit low performance in the ASR task, while replacing MHSA with BiMamba layers demonstrates impressive performance and outperforms the vanilla Transformer and Conformer models. Since the latter approach achieves significantly higher ASR performance by additionally employing a feed-forward network (FFN) and a residual connection compared to the independent Mamba and BiMamba models, we then explore the factors contributing to this performance improvement via ablation studies in Table 16.

We assume that extracting high-abstraction-level information requires greater nonlinearity than capturing low-abstraction-level information. Specifically, ASR models transcribe speech signals by understanding the context of acoustic features and aligning speech to tokens, corresponding to low-level sequential and high-level semantic information, respectively. Since a speech enhancement model focuses on low-abstraction-level spectral information, an ASR model may need higher nonlinear ability than a speech enhancement model. As illustrated in Section 2, we consider a BiMamba layer as a weakly nonlinear module similar to MHSA [55]. In Figure. 3, we use the BiMamba model to find the decision boundary for data with simple and complex distribution, respectively. We observe that BiMamba struggles to find the decision boundary for data of a complex distribution without the aid of an FFN (with ReLU activation similar to that in Transformer), which validates our assumption.

In addition, results in Table 16 indicate the effectiveness of the FFN and residual connection in a Transformer model for ASR. Similar to independent ExtBiMamba, removing the residual connection and FFN from a Transformer model leads to gradient vanishing and decreases nonlinearity, resulting in significant performance degradation for ASR. This further underpins that using BiMamba layers as a replacement for MHSA is more appropriate for speech tasks which require models to learn high-abstraction-level information than employing it independently.

7 Conclusion

In this paper, we explore the use of Mamba in speech processing, for tasks requiring information from low to high abstraction levels. We first compared two bidirectional designs for Mamba and next employed them independently or as a replacement for MHSA in Transformer and Conformer models. While independent BiMamba models exhibited high performance in the speech enhancement task with the ability to capture low-abstraction-level spectral information, it can not well achieve speech recognition, which requires semantic information within the speech signal. In contrast, using BiMamba as a replacement of MHSA in Conformer (i.e., ConExtBiMamba) matched or exceeded the performance of the SOTA Branchformer across multiple datasets. Ablation studies suggest that using BiMamba to replace MHSA is more appropriate for tasks requiring high-abstract-level information due to greater nonlinearity compared to independent BiMamba.

Limitation and Broader Impacts

There are numerous datasets for Speech Recognition and Speech Enhancement, and we cannot guarantee that our model will outperform the Conformer across all datasets. However, we have conducted experiments on a variety of datasets, including laboratory speech, multilingual speech, multilingual recordings from real-world environments, and extremely small datasets. These cover most scenarios and sufficiently demonstrate the effectiveness of our model.

Our research enhances the performance of speech recognition and speech enhancement, but more importantly, it provides guidance on how to use Mamba in the speech domain, especially in areas requiring semantic information. Potential negative impacts include further displacement of manual transcription due to improved model performance. However, currently, there are few people engaged in manual annotation, and our model also has the potential to create more job opportunities in the field of artificial intelligence.

Acknowledgement

This work was supported by the Australian Research Council Discovery Project DP230101184.

References

- [1] Ashish Vaswani, Noam Shazeer, Niki Parmar, Jakob Uszkoreit, Llion Jones, Aidan N Gomez, Łukasz Kaiser, and Illia Polosukhin. Attention is all you need. *Advances in neural information processing systems*, 30, 2017.
- [2] Alexey Dosovitskiy, Lucas Beyer, Alexander Kolesnikov, Dirk Weissenborn, Xiaohua Zhai, Thomas Unterthiner, Mostafa Dehghani, Matthias Minderer, Georg Heigold, Sylvain Gelly, et al. An image is worth 16x16 words: Transformers for image recognition at scale. In *International Conference on Learning Representations*, 2020.
- [3] Anurag Arnab, Mostafa Dehghani, Georg Heigold, Chen Sun, Mario Lučić, and Cordelia Schmid. Vivit: A video vision transformer. In *Proceedings of the IEEE/CVF international conference on computer vision*, pages 6836–6846, 2021.
- [4] Ze Liu, Yutong Lin, Yue Cao, Han Hu, Yixuan Wei, Zheng Zhang, Stephen Lin, and Baining Guo. Swin transformer: Hierarchical vision transformer using shifted windows. In *Proceedings of the IEEE/CVF international conference on computer vision*, pages 10012–10022, 2021.
- [5] Jacob Devlin Ming-Wei Chang Kenton and Lee Kristina Toutanova. Bert: Pre-training of deep bidirectional transformers for language understanding. In *Proceedings of NAACL-HLT*, pages 4171–4186, 2019.
- [6] Xiao Liu, Yanan Zheng, Zhengxiao Du, Ming Ding, Yujie Qian, Zhilin Yang, and Jie Tang. Gpt understands, too. *AI Open*, 2023.
- [7] Hugo Touvron, Louis Martin, Kevin Stone, Peter Albert, Amjad Almahairi, Yasmine Babaei, Nikolay Bashlykov, Soumya Batra, Prajjwal Bhargava, Shruti Bhosale, et al. Llama 2: Open foundation and fine-tuned chat models. *arXiv preprint arXiv:2307.09288*, 2023.
- [8] Anmol Gulati, James Qin, Chung-Cheng Chiu, Niki Parmar, Yu Zhang, Jiahui Yu, Wei Han, Shibo Wang, Zhengdong Zhang, Yonghui Wu, and Ruoming Pang. Conformer: Convolution-augmented Transformer for Speech Recognition. In *Proc. Interspeech 2020*, pages 5036–5040, 2020.
- [9] Yifan Peng, Siddharth Dalmia, Ian Lane, and Shinji Watanabe. Branchformer: Parallel mlp-attention architectures to capture local and global context for speech recognition and understanding. In *International Conference on Machine Learning*, pages 17627–17643. PMLR, 2022.
- [10] Albert Gu, Isys Johnson, Karan Goel, Khaled Saab, Tri Dao, Atri Rudra, and Christopher Ré. Combining recurrent, convolutional, and continuous-time models with linear state space layers. *Advances in neural information processing systems*, 34:572–585, 2021.

- [11] Albert Gu, Karan Goel, and Christopher Re. Efficiently modeling long sequences with structured state spaces. In *International Conference on Learning Representations*, 2021.
- [12] Ankit Gupta, Albert Gu, and Jonathan Berant. Diagonal state spaces are as effective as structured state spaces. *Advances in Neural Information Processing Systems*, 35:22982–22994, 2022.
- [13] Albert Gu, Karan Goel, Ankit Gupta, and Christopher Ré. On the parameterization and initialization of diagonal state space models. *Advances in Neural Information Processing Systems*, 35:35971–35983, 2022.
- [14] Albert Gu and Tri Dao. Mamba: Linear-time sequence modeling with selective state spaces. *arXiv preprint arXiv:2312.00752*, 2023.
- [15] Lianghai Zhu, Bencheng Liao, Qian Zhang, Xinlong Wang, Wenyu Liu, and Xinggang Wang. Vision mamba: Efficient visual representation learning with bidirectional state space model. *arXiv preprint arXiv:2401.09417*, 2024.
- [16] Yijun Yang, Zhaohu Xing, and Lei Zhu. Vivim: a video vision mamba for medical video object segmentation. *arXiv preprint arXiv:2401.14168*, 2024.
- [17] Opher Lieber, Barak Lenz, Hofit Bata, Gal Cohen, Jhonathan Osin, Itay Dalmedigos, Erez Safahi, Shaked Meir, Yonatan Belinkov, Shai Shalev-Shwartz, et al. Jamba: A hybrid transformer-mamba language model. *arXiv preprint arXiv:2403.19887*, 2024.
- [18] Xilin Jiang, Cong Han, and Nima Mesgarani. Dual-path mamba: Short and long-term bidirectional selective structured state space models for speech separation. *arXiv preprint arXiv:2403.18257*, 2024.
- [19] Kai Li and Guo Chen. Spmamba: State-space model is all you need in speech separation. *arXiv preprint arXiv:2404.02063*, 2024.
- [20] Changsheng Quan and Xiaofei Li. Multichannel long-term streaming neural speech enhancement for static and moving speakers. *arXiv preprint arXiv:2403.07675*, 2024.
- [21] Haizhou Li, Bin Ma, and Kong Aik Lee. Spoken language recognition: from fundamentals to practice. *Proc. IEEE*, 101(5):1136–1159, 2013.
- [22] Albert Gu, Tri Dao, Stefano Ermon, Atri Rudra, and Christopher Ré. Hippo: Recurrent memory with optimal polynomial projections. *Advances in neural information processing systems*, 33:1474–1487, 2020.
- [23] David E Rumelhart, Geoffrey E Hinton, and Ronald J Williams. Learning internal representations by error propagation, parallel distributed processing, explorations in the microstructure of cognition, ed. de rumelhart and j. mccllelland. vol. 1. 1986. *Biometrika*, 71:599–607, 1986.
- [24] Sepp Hochreiter and Jürgen Schmidhuber. Long short-term memory. *Neural computation*, 9(8):1735–1780, 1997.
- [25] Alec Radford, Karthik Narasimhan, Tim Salimans, Ilya Sutskever, et al. Improving language understanding by generative pre-training, 2018.
- [26] Zihang Dai, Zhilin Yang, Yiming Yang, Jaime G Carbonell, Quoc Le, and Ruslan Salakhutdinov. Transformer-xl: Attentive language models beyond a fixed-length context. In *Proceedings of the 57th Annual Meeting of the Association for Computational Linguistics*, pages 2978–2988, 2019.
- [27] Sanyuan Chen, Chengyi Wang, Zhengyang Chen, Yu Wu, Shujie Liu, Zhuo Chen, Jinyu Li, Naoyuki Kanda, Takuya Yoshioka, Xiong Xiao, et al. Wavlm: Large-scale self-supervised pre-training for full stack speech processing. *IEEE Journal of Selected Topics in Signal Processing*, 16(6):1505–1518, 2022.
- [28] Qiquan Zhang, Xinyuan Qian, Zhaoheng Ni, Aaron Nicolson, Eliathamby Ambikairajah, and Haizhou Li. A time-frequency attention module for neural speech enhancement. *IEEE/ACM Transactions on Audio, Speech, and Language Processing*, 31:462–475, 2023.

- [29] Qiquan Zhang, Meng Ge, Hongxu Zhu, Eliathamby Ambikairajah, Qi Song, Zhaoheng Ni, and Haizhou Li. An empirical study on the impact of positional encoding in transformer-based monaural speech enhancement. In *Proc. IEEE International Conference on Acoustics, Speech and Signal Processing (ICASSP)*, pages 1001–1005, 2024.
- [30] Vassil Panayotov, Guoguo Chen, Daniel Povey, and Sanjeev Khudanpur. Librispeech: an asr corpus based on public domain audio books. In *Proc. ICASSP*, pages 5206–5210, 2015.
- [31] Qiquan Zhang, Xinyuan Qian, Zhaoheng Ni, Aaron Nicolson, Eliathamby Ambikairajah, and Haizhou Li. A time-frequency attention module for neural speech enhancement. *IEEE/ACM TASLP*, 31:462–475, 2023.
- [32] David Snyder, Guoguo Chen, and Daniel Povey. MUSAN: A music, speech, and noise corpus. *arXiv preprint arXiv:1510.08484*, 2015.
- [33] Herman JM Steeneken and Frank WM Geurtsen. Description of the RSG-10 noise database. *report IZF*, 3:1988, 1988.
- [34] Fatemeh Saki and Nasser Kehtarnavaz. Automatic switching between noise classification and speech enhancement for hearing aid devices. In *in Proc. EMBC*, pages 736–739, 2016.
- [35] Fatemeh Saki, Abhishek Sehgal, Issa Panahi, and Nasser Kehtarnavaz. Smartphone-based real-time classification of noise signals using subband features and random forest classifier. In *Proc. ICASSP*, pages 2204–2208, 2016.
- [36] Qiquan Zhang, Aaron Nicolson, Mingjiang Wang, Kuldip K Paliwal, and Chenxu Wang. DeepMMSE: A deep learning approach to mmse-based noise power spectral density estimation. *IEEE/ACM TASLP*, 28:1404–1415, 2020.
- [37] J. Salamon, C. Jacoby, and J. P. Bello. A dataset and taxonomy for urban sound research. In *Proc. ACM-MM*, pages 1041–1044, 2014.
- [38] David B Dean, Sridha Sridharan, Robert J Vogt, and Michael W Mason. The QUT-NOISE-TIMIT corpus for the evaluation of voice activity detection algorithms. In *Proc. INTERSPEECH*, 2010.
- [39] Guoning Hu and DeLiang Wang. A tandem algorithm for pitch estimation and voiced speech segregation. *IEEE Transactions on Audio, Speech, and Language Processing*, 18(8):2067–2079, 2010.
- [40] Qiquan Zhang, Hongxu Zhu, Qi Song, Xinyuan Qian, Zhaoheng Ni, and Haizhou Li. Ripple sparse self-attention for monaural speech enhancement. In *Proc. ICASSP*, pages 1–5, 2023.
- [41] Aaron Nicolson and Kuldip K Paliwal. Masked multi-head self-attention for causal speech enhancement. *Speech Com.*, 125:80–96, 2020.
- [42] Recommendation ITU-T P ITU. 862.2: Wideband extension to recommendation P. 862 for the assessment of wideband telephone networks and speech codecs. ITU-Telecommunication standardization sector, 2007.
- [43] Jesper Jensen and Cees H Taal. An algorithm for predicting the intelligibility of speech masked by modulated noise maskers. *IEEE/ACM TASLP*, 24(11):2009–2022, 2016.
- [44] Yi Hu and Philipos C Loizou. Evaluation of objective quality measures for speech enhancement. *IEEE Trans. Audio, Speech, Lang. process.*, 16(1):229–238, 2007.
- [45] Alejandro Acero and Richard M Stern. Environmental robustness in automatic speech recognition. In *International Conference on Acoustics, Speech, and Signal Processing*, pages 849–852. IEEE, 1990.
- [46] Dau-Cheng Lyu, Tien-Ping Tan, Eng Siong Chng, and Haizhou Li. Seame: a mandarin-english code-switching speech corpus in south-east asia. In *Eleventh Annual Conference of the International Speech Communication Association*, 2010.

- [47] Xian Shi, Qiangze Feng, and Lei Xie. The asru 2019 mandarin-english code-switching speech recognition challenge: Open datasets, tracks, methods and results. *arXiv preprint arXiv:2007.05916*, 2020.
- [48] Zhiping Zeng, Yerbolat Khassanov, Van Tung Pham, Haihua Xu, Eng Siong Chng, and Haizhou Li. On the end-to-end solution to mandarin-english code-switching speech recognition. In *Proc. Interspeech*, pages 2165–2169, 2019.
- [49] Hexin Liu, Xiangyu Zhang, Leibny Paola Garcia, Andy WH Khong, Eng Siong Chng, and Shinji Watanabe. Aligning speech to languages to enhance code-switching speech recognition. *arXiv preprint arXiv:2403.05887*, 2024.
- [50] Suyoun Kim, Takaaki Hori, and Shinji Watanabe. Joint ctc-attention based end-to-end speech recognition using multi-task learning. In *2017 IEEE international conference on acoustics, speech and signal processing (ICASSP)*, pages 4835–4839. IEEE, 2017.
- [51] Shinji Watanabe, Takaaki Hori, Shigeki Karita, Tomoki Hayashi, Jiro Nishitoba, Yuya Unno, Nelson Enrique Yalta Soplín, Jahn Heymann, Matthew Wiesner, Nanxin Chen, Adithya Renduchintala, and Tsubasa Ochiai. ESPnet: End-to-end speech processing toolkit. In *Proceedings of Interspeech*, pages 2207–2211, 2018.
- [52] Zhifeng Kong, Wei Ping, Amrbrish Dantrey, and Bryan Catanzaro. Speech denoising in the waveform domain with self-attention. In *Proc. ICASSP*, pages 7867–7871, 2022.
- [53] Hexin Liu, Haihua Xu, Leibny Paola Garcia, Andy W. H. Khong, Yi He, and Sanjeev Khudanpur. Reducing language confusion for code-switching speech recognition with token-level language diarization. In *Proc. IEEE Int. Conf. Acoust., Speech, Signal Process.*, pages 1–5, 2023.
- [54] Hexin Liu, Leibny Paola Garcia, Xiangyu Zhang, Andy WH Khong, and Sanjeev Khudanpur. Enhancing code-switching speech recognition with interactive language biases. In *Proc. IEEE Int. Conf. Acoust., Speech, Signal Process.*, pages 10886–10890. IEEE, 2024.
- [55] Christopher Manning. Lecture 8: Transformers. CS224N: Natural Language Processing with Deep Learning, Stanford University, 2024. Accessed: 2024-05-14, Slide 32.
- [56] Ariel Ephrat, Inbar Mosseri, Oran Lang, Tali Dekel, Kevin Wilson, Avinatan Hassidim, William T Freeman, and Michael Rubinstein. Looking to listen at the cocktail party: A speaker-independent audio-visual model for speech separation. *arXiv preprint arXiv:1804.03619*, 2018.
- [57] Diederik P Kingma and Jimmy Ba. Adam: A method for stochastic optimization. *arXiv preprint arXiv:1412.6980*, 2014.
- [58] Philipp Koehn. *Neural machine translation*. Cambridge University Press, 2020.

A Algorithms of Bidirectional Mamba (InnBiMamba and ExtBiMamba)

Algorithm 1 InnBiMamba Layer Workflow

Require: $\mathbf{H}_{l-1}: (\text{B}, \text{L}, \text{D})$
Ensure: $\mathbf{H}_l: (\text{B}, \text{L}, \text{D})$

- 1: $\mathbf{H}'_{l-1}: (\text{B}, \text{L}, \text{D}) \leftarrow \mathbf{Norm}(\mathbf{H}_{l-1})$
- 2: $\mathbf{x}: (\text{B}, \text{L}, \text{E}) \leftarrow \mathbf{Linear}^{\mathbf{x}}(\mathbf{H}'_{l-1})$
- 3: $\mathbf{z}: (\text{B}, \text{L}, \text{E}) \leftarrow \mathbf{Linear}^{\mathbf{z}}(\mathbf{H}'_{l-1})$
- 4: **for** $o \in \{\text{forward}, \text{backward}\}$ **do**
- 5: $\mathbf{x}'_o: (\text{B}, \text{L}, \text{E}) \leftarrow \mathbf{SiLU}(\mathbf{Conv1d}_o(\mathbf{x}))$
- 6: $\mathbf{B}_o: (\text{B}, \text{L}, \text{N}) \leftarrow \mathbf{Linear}^{\mathbf{B}}_o(\mathbf{x}'_o)$
- 7: $\mathbf{C}_o: (\text{B}, \text{L}, \text{N}) \leftarrow \mathbf{Linear}^{\mathbf{C}}_o(\mathbf{x}'_o)$
- 8: $\mathbf{\Delta}_o: (\text{B}, \text{L}, \text{E}) \leftarrow \log(1 + \exp(\mathbf{Linear}^{\mathbf{\Delta}}_o(\mathbf{x}'_o) + \mathbf{Parameter}^{\mathbf{\Delta}}_o))$
- 9: $\mathbf{\bar{A}}_o: (\text{B}, \text{L}, \text{E}, \text{N}) \leftarrow \mathbf{\Delta}_o \otimes \mathbf{Parameter}^{\mathbf{A}}_o$
- 10: $\mathbf{\bar{B}}_o: (\text{B}, \text{L}, \text{E}, \text{N}) \leftarrow \mathbf{\Delta}_o \otimes \mathbf{B}_o$
- 11: $\mathbf{y}_o: (\text{B}, \text{L}, \text{E}) \leftarrow \mathbf{SSM}(\mathbf{\bar{A}}_o, \mathbf{\bar{B}}_o, \mathbf{C}_o)(\mathbf{x}'_o)$
- 12: **end for**
- 13: $\mathbf{y}'_{\text{forward}}: (\text{B}, \text{L}, \text{E}) \leftarrow \mathbf{y}_{\text{forward}} \odot \mathbf{SiLU}(\mathbf{z})$
- 14: $\mathbf{y}'_{\text{backward}}: (\text{B}, \text{L}, \text{E}) \leftarrow \mathbf{y}_{\text{backward}} \odot \mathbf{SiLU}(\mathbf{z})$
- 15: $\mathbf{H}_l: (\text{B}, \text{L}, \text{D}) \leftarrow \mathbf{Linear}^{\mathbf{H}}(\mathbf{y}'_{\text{forward}} + \mathbf{y}'_{\text{backward}}) + \mathbf{H}_{l-1}$
- 16: **return** \mathbf{H}_l

Algorithm 2 ExtBiMamba Layer Workflow

Require: $\mathbf{H}_{l-1}: (\text{B}, \text{L}, \text{D})$
Ensure: $\mathbf{H}_l: (\text{B}, \text{L}, \text{D})$

- 1: $\mathbf{H}'_{l-1}: (\text{B}, \text{L}, \text{D}) \leftarrow \mathbf{Norm}(\mathbf{H}_{l-1})$
- 2: **for** $o \in \{\text{forward}, \text{backward}\}$ **do**
- 3: $\mathbf{x}_o: (\text{B}, \text{L}, \text{E}) \leftarrow \mathbf{Linear}^{\mathbf{x}}_o(\mathbf{H}'_{l-1})$
- 4: $\mathbf{z}_o: (\text{B}, \text{L}, \text{E}) \leftarrow \mathbf{Linear}^{\mathbf{z}}_o(\mathbf{H}'_{l-1})$
- 5: $\mathbf{x}'_o: (\text{B}, \text{L}, \text{E}) \leftarrow \mathbf{SiLU}(\mathbf{Conv1d}_o(\mathbf{x}_o))$
- 6: $\mathbf{B}_o: (\text{B}, \text{L}, \text{N}) \leftarrow \mathbf{Linear}^{\mathbf{B}}_o(\mathbf{x}'_o)$
- 7: $\mathbf{C}_o: (\text{B}, \text{L}, \text{N}) \leftarrow \mathbf{Linear}^{\mathbf{C}}_o(\mathbf{x}'_o)$
- 8: $\mathbf{\Delta}_o: (\text{B}, \text{L}, \text{E}) \leftarrow \log(1 + \exp(\mathbf{Linear}^{\mathbf{\Delta}}_o(\mathbf{x}'_o) + \mathbf{Parameter}^{\mathbf{\Delta}}_o))$
- 9: $\mathbf{\bar{A}}_o: (\text{B}, \text{L}, \text{E}, \text{N}) \leftarrow \mathbf{\Delta}_o \otimes \mathbf{Parameter}^{\mathbf{A}}_o$
- 10: $\mathbf{\bar{B}}_o: (\text{B}, \text{L}, \text{E}, \text{N}) \leftarrow \mathbf{\Delta}_o \otimes \mathbf{B}_o$
- 11: $\mathbf{y}_o: (\text{B}, \text{L}, \text{E}) \leftarrow \mathbf{SSM}(\mathbf{\bar{A}}_o, \mathbf{\bar{B}}_o, \mathbf{C}_o)(\mathbf{x}'_o)$
- 12: $\mathbf{y}'_o: (\text{B}, \text{L}, \text{D}) \leftarrow \mathbf{Linear}^{\mathbf{H}}_o(\mathbf{y}_o \odot \mathbf{SiLU}(\mathbf{z}_o))$
- 13: **end for**
- 14: $\mathbf{H}_l: (\text{B}, \text{L}, \text{D}) \leftarrow (\mathbf{y}'_{\text{forward}} + \mathbf{y}'_{\text{backward}}) + \mathbf{H}_{l-1}$
- 15: **return** \mathbf{H}_l

Algorithms 1 and 2 illustrate the workflows of InnBiMamba and ExtBiMamba, respectively. The main differences are highlighted in violet. For the InnBiMamba layer, the linear input projections ($\mathbf{Linear}^{\mathbf{x}}$ and $\mathbf{Linear}^{\mathbf{z}}$) and the linear output projection $\mathbf{Linear}^{\mathbf{H}}$ are shared across forward and backward operations. In contrast, the ExtBiMamba layer uses different input linear projections ($\mathbf{Linear}^{\mathbf{x}}_o$ and $\mathbf{Linear}^{\mathbf{z}}_o$) and output linear projections ($\mathbf{Linear}^{\mathbf{H}}_o$) across forward and backward operations.

B Model Configurations for ASR

For Mamba and BiMamba models, we employ the default hyper-parameters [14]: the state dimension $d_{\text{state}} = 16$, convolution dimension $d_{\text{conv}} = 4$, and the expansion factor was set to 2. To keep the same batch size as in the official implementation of ESPnet, the experiments on the LibriSpeech-960 dataset

were performed on an NVIDIA A100 80GB. All the other experiments were run on an NVIDIA V100 32GB. The detailed model configurations for each dataset are given in Tables 9, 10 and 11.

Table 9: Implementation details in different tasks and datasets. We show the best Transformer configurations reported in ESPnet Official

	LibriSpeech100	LibriSpeech960	ASRU	SEAME
Frontend				
window length	400	400	400	400
hop length	160	128	160	160
SpecAug				
time warp window	5	5	5	5
num of freq masks	2	2	2	2
freq mask width	(0, 27)	(0, 30)	(0, 27)	(0, 27)
num of time masks	2	2	2	2
time mask width or ratio range	(0, 0.05)	(0, 40)	(0, 0.05)	(0, 0.05)
Architecture				
feature size d	256	512	256	256
hidden size d_{hidden}	1024	2048	1024	2048
attention heads h	4	8	4	4
num of encoder layers	18	18	18	24
depth-wise conv kernel	31	31	31	31
Training				
epochs	70	100	70	70
learning rate	2e-3	2e-3	2e-3	2e-3
warmup steps	15k	25k	15k	15k
weight decay	1e-6	1e-6	1e-6	1e-6
dropout rate	0.1	0.1	0.1	0.1
ctc weight	0.3	0.3	0.3	0.3
label smoothing weight	0.1	0.1	0.1	0.1

Table 10: Implementation details in different tasks and datasets. We show the best Conformer configurations reported in ESPnet Official

	LibriSpeech100	LibriSpeech960	ASRU	SEAME
Frontend				
window length	400	400	400	400
hop length	160	160	160	160
SpecAug				
time warp window	5	5	5	5
num of freq masks	2	2	2	2
freq mask width	(0, 27)	(0, 27)	(0, 30)	(0, 30)
num of time masks	2	2	2	2
time mask width or ratio range	(0, 0.05)	(0, 0.05)	(0, 40)	(0, 40)
Architecture				
feature size d	256	512	256	256
hidden size d_{hidden}	1024	2048	2048	2048
attention heads h	4	8	4	4
num of encoder layers	12	12	12	12
depth-wise conv kernel	31	31	31	31
Training				
epochs	120	50	70	70
learning rate	2e-3	2.5e-3	1e-3	1e-3
warmup steps	15k	40k	25k	25k
weight decay	1e-6	1e-6	1e-6	1e-6
dropout rate	0.1	0.1	0.1	0.1
ctc weight	0.3	0.3	0.3	0.3
label smoothing weight	0.1	0.1	0.1	0.1

Table 11: Implementation details in different tasks and datasets. We show the best branchformer configurations reported in ESPnet Official

	LibriSpeech100	LibriSpeech960	ASRU	SEAME
Frontend				
window length	400	400	400	400
hop length	160	160	160	160
SpecAug				
time warp window	5	5	5	5
num of freq masks	2	2	2	2
freq mask width	(0, 27)	(0, 27)	(0, 27)	(0, 27)
num of time masks	2	2	2	2
time mask width or ratio range	(0, 0.05)	(0, 0.05)	(0, 0.05)	(0, 0.05)
Architecture				
feature size d	256	512	256	256
hidden size d_{hidden}	1024	2048	2048	1024
attention heads h	4	8	4	4
num of encoder layers	12	18	12	12
depth-wise conv kernel	31	31	31	31
Training				
epochs	70	70	70	70
learning rate	2e-3	2.5e-3	2e-3	2e-3
warmup steps	15k	40k	15k	15k
weight decay	1e-6	1e-6	1e-6	1e-6
dropout rate	0.1	0.1	0.1	0.1
ctc weight	0.3	0.3	0.3	0.3
label smoothing weight	0.1	0.1	0.1	0.1

C Experiments on Speech Enhancement

C.1 Detailed Experimental Setup

Data Generation. Noise recordings that exceeded 30 seconds in duration were split into clips of 30 seconds or less. This yielded 6 809 noise clips, with each clip less than or equal to 30 seconds in duration. For validation experiments, 1 000 clean speech and noise clips (without replacement) were randomly drawn from the aforementioned clean speech and noise sets and mixed to generate a validation set of 1 000 noisy clips, where each clean speech clip was degraded by a random section of one noise clip at a random SNR level (sampled between -10 and 20 dB, in 1 dB steps). For evaluation experiments, we employed four real-world noise sources (excluded from the training set) including two non-stationary and two colored ones. The two non-stationary noise sources were the *voice babble* from the RSG-10 noise dataset [33] and *street music* from the Urban Sound dataset [37]. The two colored noise sources were *F16* and *factory welding* from RSG-10 noise dataset [33]. For each of the four noises, we randomly picked twenty clean speech clips (without replacement) from the *test-clean-100* of LibriSpeech corpus [30] and degraded each clip with a random section of the noise clip at the five SNR levels, i.e., $\{-5$ dB, 0 dB, 5 dB, 10 dB, 15 dB $\}$. This generated 400 noisy mixtures for evaluation.

Feature Extraction. All audio signals were sampled at a rate of 16 kHz. We employed a 512-sample (32 ms) long square-root-Hann window with a hop length of 256 samples (16 ms), to extract a 257-point single-sided STFT spectral magnitude as the input to the neural models [31].

Model Configurations. To perform extensive comparison studies across different model sizes, we use the Transformer and Conformer architectures comprising $N \in \{4, 6\}$ stacked Transformer and Conformer layers respectively [31]. For the Transformer speech enhancement backbone, we follow the configuration in [29, 31]: the layer dimension $d_{\text{model}} = 256$, the number of attention heads $H = 8$, and the inner-layer size of the feed-forward network (FFN) $d_{\text{ff}} = 1024$. For the Conformer backbone, we adopt the parameter configurations in [31]: the layer dimension $d_{\text{model}} = 256$, the number of attention heads $H = 8$, the kernel size of convolution 32, the expansion factor for convolution module 2, and the inner-layer size of FFN $d_{\text{ff}} = 1024$. For the Mamba model, we use the parameter configurations in [14]: the model dimension $D = 256$, the SSM state dimension $N = 16$, the local

convolution width $d_{\text{conv}} = 4$, and the expansion factor $E = 2$. All the experiments were run on an NVIDIA Tesla V100-SXM2-32GB GPU.

Implementation Details. All the models were implemented in PyTorch. We used mean-square error (MSE) on the power-law compressed spectral magnitude as the objective loss function [56]. The noisy mixtures were dynamically generated at training time. For each minibatch, we randomly picked 10 clean speech clips and degrade each clip by a random section of a random noise clip at a random SNR level sampled from -10 to 20 dB (in 1 dB steps). The *Adam* algorithm [57] was used for gradient optimization, with parameters as in [1], i.e., $\beta_1 = 0.9$, $\beta_2 = 0.98$, and $\epsilon = 10^{-9}$. We utilized the gradient clipping technique to cut the gradient values to a range between -1 and 1 . All the models were trained for 150 epochs for fair comparison. The warm-up strategy was adopted to adjust the learning rate: $lr = d_{\text{model}}^{-0.5} \cdot \min(n_{\text{step}}^{-0.5}, n_{\text{step}} \cdot w_{\text{steps}}^{-1.5})$, where n_{step} and w_{steps} denote the iteration steps and the warm-up iteration steps, respectively. We followed the study [31] and set w_{steps} as 40000.

C.2 Experiments on Mamba layer vs. MHSA

Table 12: Evaluation results for replacing the MHSA with Mamba/BiMamba layer in Transformer network, across causal and noncausal configurations.

Method	#Params Causality		Metrics					
			NB-PESQ	WB-PESQ	ESTOI	CSIG	CBAK	COVL
Noisy	–	–	1.88	1.24	56.12	2.26	1.80	1.67
Transformer-4	3.29 M	✓	2.56	1.84	70.32	3.17	2.39	2.47
– MHSA + Mamba	3.99 M	✓	2.65	1.93	72.28	3.24	2.45	2.55
Transformer-4	3.29 M	✗	2.74	2.01	73.44	3.31	2.50	2.63
– MHSA + InnBiMamba	4.17 M	✗	2.86	2.15	76.24	3.44	2.61	2.78
– MHSA + ExtBiMamba	5.74 M	✗	2.88	2.18	76.75	3.54	2.63	2.84
Transformer-6	4.86 M	✓	2.60	1.87	71.37	3.20	2.41	2.50
– MHSA + Mamba	5.92 M	✓	2.68	1.95	73.04	3.31	2.48	2.60
Transformer-6	4.86 M	✗	2.78	2.05	74.56	3.38	2.52	2.69
– MHSA + InnBiMamba	6.19 M	✗	2.89	2.17	77.22	3.49	2.61	2.80
– MHSA + ExtBiMamba	8.54 M	✗	2.91	2.21	77.60	3.60	2.65	2.88

Table 13: Evaluation results for replacing the MHSA with Mamba/BiMamba layer in Conformer network, across causal and noncausal configurations.

Method	#Params Causality		Metrics					
			NB-PESQ	WB-PESQ	ESTOI	CSIG	CBAK	COVL
Noisy	–	–	1.88	1.24	56.12	2.26	1.80	1.67
Conformer-4	6.22 M	✓	2.67	1.94	72.78	3.29	2.45	2.58
– MHSA + Mamba	6.92 M	✓	2.69	1.95	73.27	3.29	2.48	2.59
Conformer-4	6.22 M	✗	2.88	2.17	76.68	3.51	2.61	2.82
– MHSA + InnBiMamba	7.10 M	✗	2.89	2.17	77.40	3.51	2.62	2.81
– MHSA + ExtBiMamba	8.67 M	✗	2.92	2.20	77.74	3.57	2.64	2.88
Conformer-6	9.26 M	✓	2.68	1.94	73.41	3.30	2.46	2.59
– MHSA + Mamba	10.32 M	✓	2.71	1.95	73.69	3.34	2.49	2.62
Conformer-6	9.26 M	✗	2.91	2.20	77.56	3.54	2.62	2.84
– MHSA + InnBiMamba	10.59 M	✗	2.92	2.19	77.85	3.52	2.64	2.83
– MHSA + ExtBiMamba	12.94 M	✗	2.93	2.23	78.21	3.60	2.65	2.89

Table 14: Training speed and inference speed of Transformer, TranBiMamba, and Conformer and ConBiMamba.

	Transformer-6	TransInnBiMamba-6	TransExtBiMamba-6	Conformer-6	ConInnBiMamba-6	ConExtBiMamba-6
sec/step	0.125	0.155	0.161	0.215	0.206	0.214
RTF	2.12×10^{-4}	1.81×10^{-4}	1.95×10^{-4}	3.27×10^{-4}	2.85×10^{-4}	2.99×10^{-4}

D Further Explanation of Mamba used in ASR

D.1 Performance Across Different Mamba/BiMamba Sizes

Table 15 reports the performance of Mamba and BiMamba on LibriSpeech100 and SEAME, across different model sizes. With comparative model sizes, Mamba/BiMamba still performs poorly than the Conformer.

Table 15: WER/MER results (%) for LibriSpeech100 and SEAME: the left part displays results from LibriSpeech100, while the right part shows results from SEAME.

Method	#Params (M)	dev	test	#Params (M)	man	sgc
Conformer	34.23	6.3	6.5	47.27	16.9	23.6
Transformer	29.38	8.0	8.4	29.38	17.7	24.5
<i>Mamba-based Models</i>						
Mamba	20.41	40.8	40	20.41	44.5	55.3
Mamba Large	32.52	38.8	39.2	28.78	45.5	55
ExtBiMamba	25.79	38.5	37.7	25.79	44.4	55.2
ExtBiMamba Large	33.52	37.8	37.2	33.52	43.6	54.3

D.2 Ablation study of FFN and Residual for ExtBiMamba

Table 16: Ablation Studies on LibriSpeech100 for Transformer and ConExtBiMamba by WER.

Method	dev	test
Transformer	8.0	8.4
– Residual	45.7	54.8
– FFN	23.2	25.4
ExtBiMamba	38.5	37.7
+ Residual	42.1	41.7
+ FFN	34.9	36.1

D.3 InnBiMamba vs. ExtBiMamba

In Tables 8 and 17, we present the performance of InnBiMamba and ExtBiMamba in Transformer and Conformer frameworks. We found that ExtBiMamba consistently outperforms InnBiMamba across all datasets. Given that InnBiMamba typically has fewer parameters than ExtBiMamba, we increase the number of layers with InnBiMamba to match ExtBiMamba for fair comparison. Again, ExtBiMamba performs better than InnBiMamba.

Table 18 compares the training and inference speeds of Conformer, ConInnBiMamba, and ConExtBiMamba. The results show that ConInnBiMamba and ConExtBiMamba train and infer faster than the Conformer, confirming the training and inference efficiency of the ConBiMamba architectures. Among them, ConInnBiMamba is slightly faster than ConExtBiMamba.

Table 17: InnBiMamba vs. ExtBiMamba: MER Results (%) on ASRU and SEAME, Left results are from ASRU, Right results are from SEAME

Method	Params (M)	dev	test	Params (M)	man	sgc
Transformer	30.86	13.7	13.1	29.86	17.7	24.5
– MHSA + InnBiMamba	34.80	20.2	19.5	33.81	18.4	26.0
– MHSA + ExtBiMamba	44.24	18.7	18	43.25	17.2	24.3
Conformer	48.27	12.8	12.2	47.27	16.9	23.6
– MHSA + InnBiMamba	50.10	12.7	12.2	49.11	17.1	23.8
– MHSA + ExtBiMamba	56.40	12.3	11.5	55.40	16.6	23.4

Table 18: Training speed (mins/epoch) and Inference speed (RTF) for ASR in LibriSpeech100 on NVIDIA Tesla V100.

	Conformer	ConInnBiMamba	ConExtBiMamba
mins/epoch	21.4	18.3	19.8
RTF	0.179	0.174	0.177

E Ablation Study on ConExtBiMamba for ASR Task

E.1 Effect of Hyper-Parameter for BiMamba in ConExtBiMamba

The default hyper-parameters for ConExtBiMamba are defined as: the SSM state dimension $d_{\text{state}} = 16$, the state expansion factor $E = 2$, and the local convolution width $d_{\text{conv}} = 4$. From Table 19, we find that increasing the state expansion factor or decreasing the local convolution width has little impact on the performance of ConExtBiMamba.

We further investigate the impact of the A matrix on performance. The A matrix plays a crucial role in both S4 and Mamba. In the original Mamba paper, it is initialized using a real-valued diagonal matrix. However, ensuring randomness is important in deep learning [58]. To explore this, we examine three types of A matrices: a real-valued diagonal matrix, a completely randomized matrix, and a real-valued diagonal matrix initialized by multiplying each element with noise generated from a Gaussian distribution. Through our experiments, we discovered that the diagonal matrix with Gaussian noise yielded the best results.

Table 19: Ablation Study on LibriSpeech100 for ConExtBiMamba by employing WER (%)

Method	dev (↓)	dev other (↓)	test (↓)	test other (↓)
ConvExtBiMamba with Gaussian Noise	5.9	17.1	6.0	17.3
→ $d_{\text{state}} = 32$	5.9	17.1	6.0	17.3
→ $d_{\text{conv}} = 2$	6.0	17.1	6.2	17.3
→ $E = 4$	5.9	17.1	6.0	17.3
→ Random Noise A matrix	6.0	17.2	6.2	17.4
→ default A matrix	6.1	17.2	6.2	17.5

E.2 Effect of Hyper-Parameters for ConExtBiMamba

We conduct ablation experiments on Swish Activation, Macaron-style feed-forward layers, positional encoding, and dropout. From Table 20, it is apparent that Swish Activation and Macaron-style feed-forward layers enhance the model’s performance, while positional encoding and dropout do not have a significant impact. We suggest that the reason positional encoding, a crucial component in Transformer-based models, does not significantly affect the ConExtBiMamba model is twofold. Firstly, Mamba independently models each input, which suggests that the model may better differentiate between different positions. Secondly, because Mamba operates similarly to an RNN, the dependencies between inputs inherently embed some positional information into the model, thus diminishing the impact of positional encoding.

Table 20: Ablation Studies for ConExtBiMamba on LibriSpeech100.

Method	dev (↓)	dev other (↓)	test (↓)	test other (↓)
ConExtBiMamba	5.9	17.1	6.0	17.3
– Macaron	6.1	17.7	6.3	17.9
– Swish	6.2	17.7	6.4	18.1
– Dropout	6.0	17.1	6.0	17.4
+ Positional Encoding	6.0	17.1	6.0	17.3

E.3 Performance on Extremely Small Datasets

To evaluate model robustness, we conduct tests on the AN4 dataset—a notably small dataset—using five randomly selected seeds for both the Conformer and ConExtBiMamba models under identical hyperparameters. Our results show that ConExtBiMamba consistently outperforms the Conformer across all seeds. Specifically, the mean WER for the Conformer was 10.02, while it was significantly lower for ConExtBiMamba at just 4.54. Remarkably, ConExtBiMamba also demonstrated exceptional robustness, with a WER variance of only 1.11 compared to the Conformer’s substantially higher variance of 77.71. Observing the loss metrics, we noted that ConBiMamba is less prone to overfitting on small datasets compared with the Conformer. This suggests that ConBiMamba, like RNNs, benefits from its ability to process information recursively over time, updating only a small set of parameters with each iteration, which helps prevent overfitting in scenarios with limited data. Additionally, this framework also avoids the gradient vanishing and explosion issues typically associated with RNNs. Combining these observations with our main results, we can conclude that ConExtBiMamba effectively merges the strengths of self-attention-based models and RNN models.

Table 21: Performance on extremely small dataset AN4 by employing WER (%)

Method/Seed	2048	233	666	1024	3407	Average	Variance
Conformer	4.0	8.2	6.1	4.4	27.4	10.02	77.71
ConExtBiMamba	3.8	3.8	4.8	3.8	6.5	4.54	1.11